Int J Adv Manuf Technol (2016) 86:2759–2770
DOI 10.1007/s00170-016-8385-y

ORIGINAL ARTICLE

A micro-model of the material removal depth for the polishing process

Junde Qi[1] · **Dinghua Zhang**[1] · **Shan Li**[1] · **Bing Chen**[1]

Received: 19 August 2015 / Accepted: 13 January 2016 / Published online: 29 January 2016

Abstract In this paper, a prediction model of the material removal depth for the polishing process is developed from the microscopic point of view. Based on the statistics analysis, and by the use of the elastic contact theory and the plastic contact theory, the relationship between the pressure and the depth of indentation is obtained. Moreover, the calculation equation for the linear removal intensity, which is the material removal depth per unit contact length along the polishing path, is presented. Finally, by integrating the linear removal intensity, the micro-model of the material removal depth for the polishing process is developed. Analyzed from the perspective of the abrasive grains, the model takes the grit designation and the structural number as the two basic variables for abrasive grains characteristics, and it is assumed that the shape of an abrasive grain is conic with spherical tip and the distribution of its protrusion heights is taken to be Gaussian distribution, which fully takes into account the impact of the abrasive grains characteristics on the depth of removal. In the model, different stages of the polishing process are decomposed in detail, and the reality that the plastic deformation is accompanied by the presence of elastic deformation is taken into consideration, which makes the model more realistic. Experimental results are compared with the prediction results to verify the theoretical model. The model can be used as the theoretical foundation for the selection of abrasive grains and the process parameters.

✉ Junde Qi
qijunde@mail.nwpu.edu.cn

[1] Key Laboratory of Contemporary Design and Integrated Manufacturing Technology of Ministry of Education, Northwestern Polytechnical University, Xi'an 710072, China

Keywords Polishing · Abrasive grains · Statistics analysis · Elastic-plastic deformation · Removal depth

1 Introduction

Polishing is a kind of finishing process that can effectively eliminate or reduce the processing defects caused by former manufacturing procedures and improve the surface quality and form accuracy, which makes it a vital role to ensure the product quality and the service life. However, most of the polishing works still rely highly on manual operations by skilled workers, which make it inefficient and difficult to ensure product consistency. It has been reported that according to statistics in the mold processing, about 37 to 50 % of the total manufacturing time is spent on polishing. Therefore, it has become a hot topic in the field of engineering and academics on how to achieve the automation of polishing and improve polishing efficiency and quality [1–4].

In the research of polishing automation, a critical and difficult problem is how to precisely control the removal of the material, namely the quantitative removal of material, so as to achieve the required form accuracy [5]. There are a number of factors in the polishing process that can affect the removal of the material, including process parameters [6, 7] such as the tool speed, the feed rate and the given pressure, as well as the characteristics of the tool such as the grain size, material, and density. In addition, most of the application workpieces are free-form surfaces which add more difficulties to the quantitative removal of material. The nature of quantitative removal of material lies in the control of removal depth of various positions on the workpiece surface. Therefore, it is obviously necessary to study the removal depth of the workpiece surface.

Currently, the most commonly used method is to develop a model of material removal depth based on Preston's equation [8, 9], which defines that the material removal depth per unit time is proportional to the instantaneous velocity and pressure. The effect of other factors (such as processing materials, polishing tools, etc.) is considered to be a proportional constant K. In other words, Preston's equation creates a linear relationship between the material removal depth and pressure as well as instantaneous velocity [10–12]. This kind of model is simple and needs a small amount of calculations. However, the determination of the proportional constant K is complicated and needs lots of experiments, once the experimental conditions change, K needs to be corrected. In addition, Preston's equation is a kind of macroscopic model and lacks of the effect of abrasive grains characteristics on the depth of removal. Most experimental and theoretical studies have shown that the characteristics of abrasive grains have an important influence on the removal depth of material [13, 14].

Therefore, from the perspective of abrasive grains, some scholars carried out many microscopic researches in the polishing process mainly concentrated on the complex interactions between the abrasive grains and the workpiece involving scratching, plowing, cutting and so on. Microscopic researches from the perspective of abrasive grains contribute to a better understanding of the mechanism of polishing. Wu et al. [14] developed a theoretical equation of the removal depth from the aspect of abrasive grains, and its solving process was discussed. Wang et al. [15] took the size of abrasive grains as an important aspect on the removal depth and developed an equation describing the relationship between the pressure and the cutting depth, and finally, the model of the linear removal intensity was presented. Both of the above two models are developed from the micro perspective, however, in the state of the plastic deformation, the elastic deformation was not considered. While in the actual polishing process, the plastic deformation is accompanied by the presence of elastic deformation [16]. Therefore different stages of the abrasive polishing process need to be decomposed in detail to make the prediction model more realistic.

In this paper, a model of predicting the material removal depth of the workpiece surface for the polishing process is developed and an approach to achieve the material removal profile is presented. Based on the statistics analysis, and by the use of the elastic contact theory and the plastic contact theory, the relationship between the pressure and the depth of indentation is obtained from the microscopic point of view. The depth of the material removal can be obtained by integrating the linear removal intensity along the polishing contact path. In this model, the effect of the abrasive grains characteristics on the removal depth is taken into account and different stages of the polishing process are decomposed in detail. Finally experimental results are compared with the prediction results to verify the theoretical model.

2 Modeling

According to the removal principle, polishing process can be mainly categorized into three groups: mechanical polishing, chemical polishing and chemical-mechanical polishing (CMP) [17]. The latter two more focus on the action of a "chemical tooth", i.e., the chemical interaction between abrasives, surface, polishing pad and carrier medium. In this paper, the method of mechanical polishing is concerned.

Mechanical polishing is a very gentle abrasive action between the grain and the workpiece to ensure a very small scratch depth. There are a large number of grains on the surface of the abrasive tool and an abrasive grain is a hard, tough substance containing many sharp projection cutting edges or points. In the polishing process, pressure is applied on the abrasive through a conformable pad or soft cloth and makes the abrasive penetrate into the surface and cut away material [18].

Therefore, in order to establish the model from the microscopic level, two parameters are considered in this paper. They are the number of abrasive grains involved in the removal of material per unit time per unit area and the volume removed by a single abrasive grain. The product of the two parameters determines the total removal volume of the material and then the material removal depth could be obtained.

2.1 The number of the effective grains

Researches and experiments show that the heights of the abrasive protrusion are not the same [15]. Therefore, only a part of grains will participate in the polishing process and this kind of grains are called the effective grains which will actually determine the removal depth of the material.

2.1.1 The number of the whole abrasive grains

In this paper, the structural number and the grit designation are taken as the two basic variables for abrasive characteristics. An abrasive tool is composed of abrasive grains, bond and air vent. The structure number S stands for the volume ratio of the grains in the whole element volume. The relationship of S and volume ratio is obtained as follows [19]:

$$V_g = 2(31-S) \tag{1}$$

where V_g (%) is the grain ratio. For instance: V_g is 62 when $S=0$, and 44 when $S=9$.

The grit designation (generally indicated by M) is used to characterize the dimension d of the abrasive grains. By fitting the data in Table 1, the corresponding relationship of M and the dimension d can be calculated as follows [19]:

$$d_m = 68M^{-1.4} \tag{2}$$

$$d_{\max} = 15.2M^{-1} \tag{3}$$

Table 1 Values of d_m, d_{max}, and σ for different grit designations [15]

M	d_{max} (10^{-3} mm)	d_m (10^{-3} mm)	σ (10^{-3} mm)
100	150	137.5	4.17
120	125	115.5	3.17
150	106	90.5	5.17
180	90	76.5	4.5
220	75	64	3.67
W40	40	34	2

where d_m is the average dimension and d_{max} is the maximum dimension of the abrasive grains.The number of the abrasive grains per unit area can be calculated as [20]:

$$N = \frac{6 \times V_g}{\pi {d_m}^2} \tag{4}$$

Eq. (4) indicates that the structural number S and the grit designation M together determine the total number of the abrasive grains per unit area. From Eqs. (1), (2), (3), and (4), the total number can be obtained in the following form:

$$N = \frac{0.03(31-S)}{\left(34^2\right)\pi M^{-2.8}} \tag{5}$$

2.1.2 Model of the heights of the abrasive protrusion

Massive experiments and researches have shown that d_{max} and d_m are very close to the maximum and the average heights of the abrasive protrusion, respectively [7], as shown in Fig. 1. The distribution of the heights of the abrasive protrusion is taken to be Gaussian distribution [21], i.e.,

$$f(h) = \frac{1}{\sqrt{2\pi}\sigma} e^{\frac{-h^2}{2\sigma^2}} \quad |h| \le 3\sigma \tag{6}$$

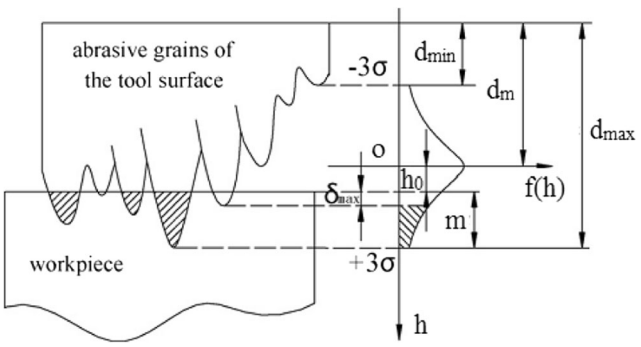

Fig. 1 Schematic diagram of the heights distribution of the abrasive protrusion

In the equation above, h is the height of the abrasive protrusion; σ is the standard deviation which can be given by:

$$\sigma = \frac{(d_{max}-d_m)}{3} \tag{7}$$

where d_m, d_{max} and σ for different grit designations are shown in Table 1.

Figure. 1 is a schematic diagram of the protrusion heights distribution in the abrasive tool surface and the origin point of the coordinate system is fixed on the horizontal position of d_m. In Fig. 1, d_{min} is the minimum dimension of the abrasive grains, h_0 is the vertical distance between the origin point and the workpiece surface, δ_{max} is the maximum overlap of elastic contact, m is the indentation depth of the highest grain. From the geometric relationship, h_0 can be expressed as follows:

$$h_0 = 3\sigma - m \tag{8}$$

where m belongs to $[0, 6\sigma]$.

2.1.3 The number of the effective grains

Through the above analysis, we can conclude that in the polishing process, not all the grains are involved in the polishing process. As shown in Fig. 1, a grain would contact with the workpiece only when the protrusion height is bigger than h_0, and the material removal process will happen only when the protrusion height is bigger than $\delta_{max} + h_0$.

Under the assumption of Hertzian contact, the geometric shape of the contact between the tool and the workpiece is elliptical [15]. As shown in Fig. 2, when the center of the contact ellipse lies in point O of polishing path, there exits infinitesimal G in the contact region of the workpiece surface, the length and width of which are dy and dx. The rotation speed of the polishing tool and

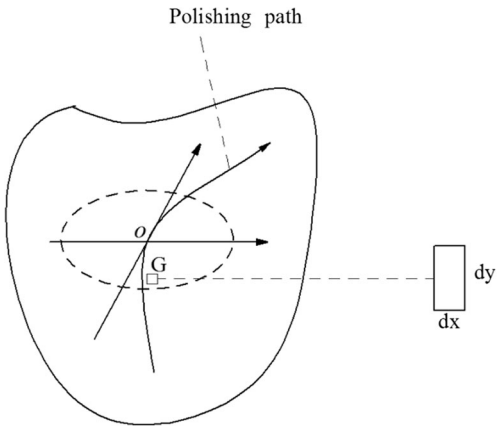

Fig. 2 Schematic diagram of the contact area between the tool and the workpiece

the feed speed of the workpiece are defined by V_t and V_f, respectively. The contact area of the workpiece at G in the time dt is:

$$S = \mathrm{dydx} = V_f \mathrm{dxdt} \tag{9}$$

And the contact area of the polishing tool at G in the time dt can be calculated as:

$$S_1 = \mathrm{dldx} = V_s \mathrm{dxdt} \tag{10}$$

where $V_s = V_t \pm V_f$ is the relative velocity between the polishing tool and the workpiece. When the direction of the feed rate is the same as that of the tool rotation, "–" is chosen, otherwise "+" is chosen.

From Eqs. (5), (6), and (10), the number of the abrasive grains that can contact with the workpiece is obtained in the following form:

$$N_1 = S_1 N \int_{h_0}^{3\sigma} f(h)dh \tag{11}$$

The number of effective grains that can actually remove the material can be calculated as:

$$N_2 = S_1 N \int_{h_0+\delta_{\max}}^{3\sigma} f(h)dh \tag{12}$$

2.2 The removal model of a single abrasive grain

In addition to the number of the effective grains, the volume removed by a single abrasive grain is another important variable influencing the material removal depth. The polishing process is a complex material removal process involving rubbing, scratching, plowing and cutting as shown in Fig. 3. The behavior of material deformation can be divided into two phases: the elastic deformation and the plastic deformation. The transition between the two phases depends on the cutting depth of an abrasive grain. Therefore, in this section two kinds of deformations are analyzed in detail and the theory of contact mechanics and the force equilibrium are used to obtain the relationship between the pressure and the depth of indentation. And finally, the removal model of a single abrasive grain is developed.

The transverse shape of the grooves produced by abrasive grains has been assumed to be triangular in most of the models developed so far [14, 15]. In reality, a single abrasive grain typically has a lot of tiny cutting edges on its tip, which is similar to a multiple-point circular arc. Experiments conducted by Lal and Shaw [22] with a single abrasive grain indicate that the grain tip could be better approximated by circular arc. Therefore, in this paper the shape of abrasive grains is assumed to be conic with spherical tip which means that the transverse shape is conic when the cutting depth is big, while the transverse shape is spherical when the cutting depth is small.

2.2.1 Elastic deformation

According to the elastic mechanics theory, for a single abrasive grain, when a normal force F_0 is applied on the workpiece, as shown in Fig. 4, then, we can get the following parameters [24]:

$$r = \left(\frac{3RF_0}{4E^*}\right)^{1/3} \tag{13}$$

$$\delta = \left(\frac{9F_0^2}{16RE^{*2}}\right)^{1/3} \tag{14}$$

$$p_0 = \frac{1}{\pi}\left(\frac{16E^{*2}F_0}{9R^2}\right)^{1/3} \tag{15}$$

$$\frac{1}{E^*} = \frac{1-\nu_3^2}{E_3} + \frac{1-\nu_2^2}{E_2} \tag{16}$$

In these equations, R is the spherical radius of the abrasive grains' tip as shown in Table 2, r is the radius of the circular contact area; δ is the overlap of elastic contact; p_0 is the mean contact pressure; E^* is the contact

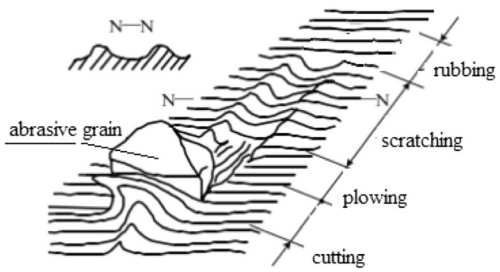

Fig. 3 Schematic diagram of the material removal by a single abrasive grain

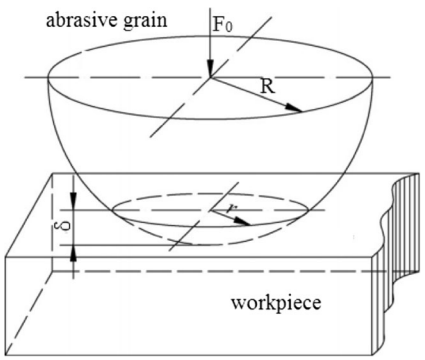

Fig. 4 Schematic diagram of a single abrasive grain acted on the workpiece

Table 2 Values of R for different grit designations [15]

M	46	60	80	W40	W28
$R(10^{-3}$ mm)	28	18	13	4	2.7

modulus of the abrasive grain and workpiece, E_2 and E_3 are Young's modulus of the workpiece and the abrasive grain, v_2 and v_3 are Poisson's ratios of the workpiece and the abrasive grain, respectively.

According to the elastic-plastic deformation theory, there will be plastic deformation on the workpiece surface when the mean contact pressure is bigger than $H_B/3$ [15, 23], where is the Brinell hardness of the workpiece surface; otherwise there is only elastic deformation on the workpiece surface without material removal. From Eqs. (14), (15), and (16), the maximum overlap of elastic contact $\delta_{\max}$ can be presented as:

$$\delta_{\max} = \frac{\pi^2 R H_B^2}{16 E^{*2}} \tag{17}$$

Therefore, when the height of the abrasive protrusion belongs to $[h_0\ ,\ h_0+\delta_{\max}]$, there is only elastic deformation on the workpiece surface, and the number of abrasive grains per unit area can be calculated as:

$$N_t = N \int_{h_0}^{h_0+\delta_{\max}} f(h)dh \tag{18}$$

From Eq. (14), solving for F_0 yields:

$$F_0 = \frac{4E^* R^{1/2}(h-h_0)^{3/2}}{3} \tag{19}$$

The force F_t producing the elastic deformation per unit area can be obtained from Eqs. (18) and (19), and it is shown as follows:

$$F_t = N_t F_0 = \frac{4NE^*\sqrt{R}}{3\sigma\sqrt{2\pi}} \int_{h_0}^{h_0+\delta_{\max}} (h-h_0)^{3/2} e^{\frac{-h^2}{2\sigma^2}} dh \tag{20}$$

2.2.2 Plastic deformation

From the analysis in Section 2.2.1, it is known that there will be plastic deformation on the workpiece surface when the height of the abrasive protrusion is bigger than $\delta_{\max}+h_0$

As we have mentioned at the beginning of section 2.2, the transverse shape is different as the cutting depth varies. Therefore, the plastic deformation is divided into two phases in this part.

1. The phase of spherical cutting

   When the cutting depth is smaller than the spherical radius of the abrasive grain's tip, the process of spherical cutting will happen. In the actual polishing process, the plastic deformation is always accompanied by the presence of elastic deformation as shown in Fig. 5. According to the elastic-plastic deformation theory, the depth of elastic deformation can be expressed as [25]:

$$\delta_c = \left(\frac{0.6\pi H_B}{2E^*}\right)^2 R \tag{21}$$

where δ_c is the depth of elastic deformation.And the corresponding force caused by the elastic deformation is as follows [25]:

$$F_c = \frac{4}{3} E^* \sqrt{R} \delta_c^{3/2} \tag{22}$$

Here, if we denote δ_p as the depth of removal, then the corresponding force caused by the plastic deformation can be calculated as [19]:

$$F_p = 2H_B \pi R \delta_p \tag{23}$$

From Eqs. (22) and (23), the total force for a single abrasive grain in the phase of spherical cutting is given by:

$$F_1 = F_c + F_p = \frac{4}{3} E^* \sqrt{R} \delta_c^{3/2} + 2H_B \pi R \Delta_h \tag{24}$$

where $\Delta_h = (h - h_0 - \delta_c)$.

As shown in Fig. 5, u_1, u_2, u_3, u_4, and u_5 are the spots on the spherical part of the abrasive grain and O is the center. The part $u_1u_2u_5$ is the elastic deformation.

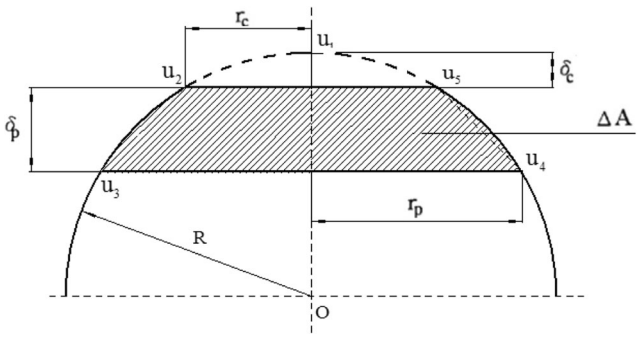

Fig. 5 Schematic diagram of the spherical cutting of a single abrasive grain

The part $u_2u_3u_4u_5$ in the area of oblique lines is the transverse shape of the cutting and its area is represented by ΔA which will be calculated in the following section. r_c and r_p are the radii of the top and bottom contact circular of the abrasive grain.

From Eqs. (12) and (24), the total force per unit area in the phase of spherical cutting can be calculated as:

$$F_{s1} = N_{21}F_1 = \frac{4\sqrt{R}\delta_c^{3/2}NE^*}{3\sigma\sqrt{2\pi}}\int_{h_0+\delta_{\max}}^{h_0+R} e^{\frac{-h^2}{2\sigma^2}}dh + \frac{2H_B\pi RN}{\sqrt{2\pi}\sigma}\int_{h_0+\delta_{\max}}^{h_0+R} e^{\frac{-h^2}{2\sigma^2}}\Delta_h dh \tag{25}$$

where N_{21} is the number of grains participating in the spherical cutting.

2. The phase of conic cutting

When the cutting depth is bigger than the spherical radius of the abrasive grain's tip, the process of conic cutting will happen and the cross-section of the removed material is shown in Fig. 6. In this phase, the elastic deformation will also occur. It is known from Eq. (21) that the elastic deformation is merely a function of R and it will not vary as the cutting depth changes. Therefore the depth and force caused by the elastic deformation are the same in the phase of spherical cutting and conic cutting.

In the phase of conic cutting, the pressure caused by the plastic deformation is always set to be $p_1 = H_B/2$ [15, 23]. It is found that the shape of the contact area is circular [15], the radius of which is equal to $(h-h_0)\tan(\alpha/2)$, where α is the apical angle of the cone. Therefore, the contact area can be expressed as:

$$S_{s2} = \pi r^2 = \pi(h-h_0)^2\tan^2\frac{\alpha}{2} \tag{26}$$

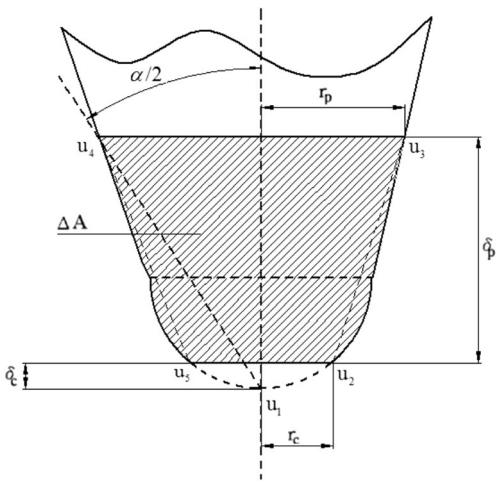

Fig. 6 Schematic diagram of the conic cutting of a single abrasive grain

Thus, the total force per unit area caused by the plastic deformation in the phase of conic cutting is presented as:

$$F_{s2} = N_{22}(F_c + S_{s2}p_1) = \frac{4\sqrt{R}\delta_c^{3/2}NE^*}{3\sigma\sqrt{2\pi}}\int_{h_0+R}^{3\sigma} e^{\frac{-h^2}{2\sigma^2}}dh + \frac{H_B\pi N\tan^2\frac{\alpha}{2}}{2\sqrt{2\pi}\sigma}\int_{h_0+R}^{3\sigma} e^{\frac{-h^2}{2\sigma^2}}(h-h_0)^2dh \tag{27}$$

where N_{22} is the number of grains participating in the conic cutting.

From Eqs. (25) and (27), the total force per unit area caused by the plastic deformation of two phases can be obtained by:

$$\begin{aligned} F_s &= F_{s1} + F_{s2} \\ &= \frac{4\sqrt{R}\delta_c^{3/2}NE^*}{3\sigma\sqrt{2\pi}}\int_{h_0+\delta_{\max}}^{3\sigma} e^{\frac{-h^2}{2\sigma^2}}dh + \frac{2H_B\pi RN}{\sqrt{2\pi}\sigma}\int_{h_0+\delta_{\max}}^{h_0+R} e^{\frac{-h^2}{2\sigma^2}}\Delta_h\ dh \\ &\quad + \frac{H_B\pi N\tan^2\frac{\alpha}{2}}{2\sqrt{2\pi}\sigma}\int_{h_0+R}^{3\sigma} e^{\frac{-h^2}{2\sigma^2}}(h-h_0)^2dh \end{aligned} \tag{28}$$

2.2.3 Indentation depth of the abrasive grains

Based on the analysis above, the total force per unit area (i.e., the pressure) mainly consists of two parts, which are the forces of the elastic deformation and the plastic deformation.

From Eqs. (20) and (28), we can see that the pressure is a function of h_0. As we know, the transition between the elastic deformation and the plastic deformation depends on the penetration depth m; therefore, according to Eq (8), h_0 is replaced by m; then the following three situations are contained between abrasive grains and workpiece:

1. When $0 \le m \le \delta_{\max}$, there is only the elastic deformation and the pressure is given by:

$$P = F_t \tag{29}$$

2. When $\delta_{\max} \le m \le R$, the elastic deformation and the plastic deformation (spherical cutting) will occur simultaneously and the pressure can be calculated as:

$$P = F_t + F_{s1} \tag{30}$$

3. When $R \le m \le 6\sigma$, the elastic deformation and the plastic deformation (spherical cutting and conic

cutting) will occur simultaneously and the pressure can be calculated as:

$$P = F_t + F_{s1} + F_{s2} \tag{31}$$

Based on the above analysis, in case of a known pressure distribution, the cutting depth of the abrasive grains could be solved.

In this paper, the contact area between the tool and the workpiece surface is assumed to be elliptic according to the Hertzian contact theory [11, 23]. The pressure distribution equation is shown in the appendix.

2.2.4 The removal volume of a single grain

The elastic deformation of the workpiece does not lead to material removal, while the plastic deformation does. Therefore, the model of the removal volume of a single grain is developed in the phase of plastic deformation.

The removal shape of the cross-section is assumed to be trapezoidal for simplification in this paper.

According to Figs. 5 and 6, the trapezoidal cross-sectional area ΔA is given by:

$$\Delta A = \left(r_c + r_p\right)\delta_p \tag{32}$$

According to the relationship of geometry:

$$r_c^2 + (R - \delta_c)^2 = R^2 \tag{33}$$

It is obtained as follows:

$$r_c^2 = 2R\delta_c - \delta_c^2 \tag{34}$$

Here, the parameters in Table 3 are adopted to calculate the following formula:

$$\frac{\delta_c^2}{2R\delta_c} = \frac{\delta_c}{2R} = 0.045\left(\frac{\pi H_B}{E^*}\right)^2 \approx 4*10^{-5} \tag{35}$$

Then we can find that $\delta_c^2 \ll 2R\delta_c$ and can be neglected, so Eq. (34) can be simplified as follows:

$$r_c^2 = 2R\delta_c \tag{36}$$

Then it results as follows:

$$r_c = \sqrt{2R\delta_c} \tag{37}$$

When it comes to r_p, two situations are discussed according to the cutting depth.

- When it is in the phase of spherical cutting, by the same token with r_c, r_p can be obtained as follows:

$$r_{p1} = \sqrt{(h - h_0)(2R - h + h_0)} \tag{38}$$

- When it is in the phase of conic cutting, following the analysis in Section 2.2.2, it is known that:

$$r_{p2} = (h - h_0)\tan\frac{\alpha}{2} \tag{39}$$

After all the parameters are obtained, the removal volume of a single grain can be expressed as V_{01} and V_{02} for spherical cutting and conic cutting correspondingly:

$$V_{01} = \Delta A_1 \mathrm{dy} = \left[\sqrt{2R\delta_c} + r_{p1}\right]\Delta_h \mathrm{dy} \tag{40}$$

$$V_{02} = \Delta A_2 \mathrm{dy} = \left[\sqrt{2R\delta_c} + r_{p2}\right]\Delta_h \mathrm{dy} \tag{41}$$

2.3 The linear removal intensity of the material

Based on the analysis of Section 2.1 and 2.2, the total removal volume of workpiece at infinitesimal G by the polishing tool in the time dt can be expressed as:

$$V = \mathrm{dxdydz} = N_2 V_0 = \frac{S_1 N}{\sqrt{2\pi}\sigma}\left(\int_{h_0+\delta_{\max}}^{h_0+R} e^{\frac{-h^2}{2\sigma^2}}\Delta A_1 \mathrm{dh} + \int_{h_0+R}^{3\sigma} e^{\frac{-h^2}{2\sigma^2}}\Delta A_2 \mathrm{dh}\right)\mathrm{dy} \tag{42}$$

Table 3 The adapted process parameters [23]

Items	Conditions
Grains	Material: A356 alloys, $M = 240$, $E_3 = 400$GPa, $V_3 = 0.3$, $\alpha = 90°$, $R = 2.792$ μm,
Tool	$E_1 = 25$ MPa, $V_1 = 0.10$, $r_1 = 50$ mm, $r_1' = \infty$, $S = 0$
Workpiece	$E_2 = 72.4$GPa, $V_2 = 0.33$, $r_2 = 20$ mm, $r_2' = 100$ mm, $H_B = 686$ MPa
Other parameters	$\gamma = 0°$, $F = 10$, 15, 20 N, $V_f = 0.105$, 0.157, 0.209, 0.262 m/min, $V_t = 7.540$, 8.561, 9.582 m/min

where dz is the removal depth at infinitesimal G.From Eqs. (9), (10), (12) and (42), we could get the following equation:

$$H_l = \frac{\mathrm{dz}}{\mathrm{dy}} = \frac{N_2 V_0}{\mathrm{dxdydy}} = \frac{S_1 N}{S\sqrt{2\pi}\sigma}(\mathrm{RV}_1 + \mathrm{RV}_2) = \frac{V_s N}{V_f \sqrt{2\pi}\sigma}(\mathrm{RV}_1 + \mathrm{RV}_2) \quad (43)$$

where RV_1 and RV_2 stand for the removal volume by the spherical cutting and conic cutting, respectively, which can be given by:

$$\mathrm{RV}_1 = \int_{h_0+\delta_{\max}}^{h_0+R} e^{\frac{-h^2}{2\sigma^2}} \Delta A_1 \mathrm{dh}$$

$$\mathrm{RV}_2 = \int_{h_0+R}^{3\sigma} e^{\frac{-h^2}{2\sigma^2}} \Delta A_2 \mathrm{dh}$$

H_l is defined as the linear removal intensity, which is the material removal depth of per unit contact length in the contact region between the polishing tool and the workpiece.

The removal depth at infinitesimal G in the contact region between the polishing tool and the workpiece can be obtained by integrating H_l along the polishing contact path, i.e.,

$$H = \int_{L_1}^{L_2} H_l \mathrm{dl} \quad (44)$$

where H is the removal depth at infinitesimal G, L_1 and L_2 are the start point and end point of the polishing contact path as shown in Fig. 7.

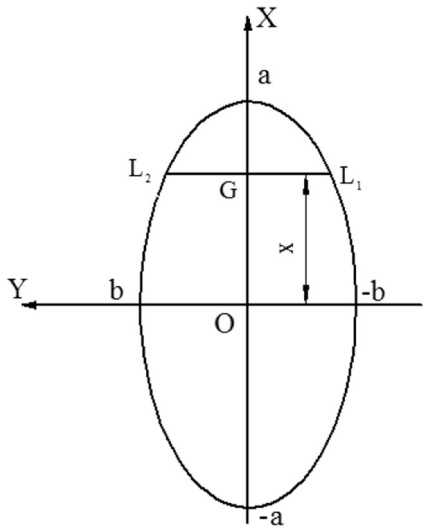

Fig. 7 Schematic diagram of the elliptic contact area between the polishing tool and the workpiece

According to the Hertzian contact theory, the contact area between the polishing tool and the workpiece is an ellipse and the boundary line of the elliptic area can be given by [11]:

$$\frac{x^2}{a^2} + \frac{y^2}{b^2} = 1 \quad (45)$$

where a and b are the semi-major axis and the semi-minor axis, respectively, which can be obtained in the appendix. As shown in Fig. 7, Y stands for the path direction and x is the distance from infinitesimal G to the center point O. As the distance x is known, the values of L_1 and L_2 can be calculated by Eq. (45).

The calculating steps of the material removal depth are shown in Fig. 8.

3 Model analysis

The relationship between dy and V_f can be expressed as follows:

$$\mathrm{dy} = V_f \mathrm{dt} \quad (46)$$

Substituting Eq. (46) into Eq. (43) and it is obtained as follows:

$$H_t = \frac{\mathrm{dz}}{\mathrm{dt}} = \frac{\mathrm{dz}}{\mathrm{dy}} \times V_f = H_l \times V_f = \frac{N}{\sqrt{2\pi}\sigma} \times (\mathrm{RV}_1 + \mathrm{RV}_2) \times V_s \quad (47)$$

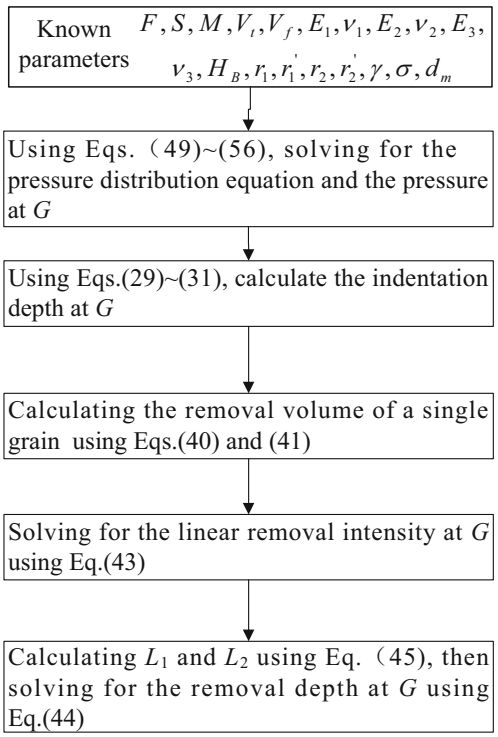

Fig. 8 The calculating steps of the material removal depth

where H_t is defined as the material removal depth per unit time at infinitesimal G.

In Eq. (47), $\frac{N}{\sqrt{2\pi}\sigma}$ is determined by the grit designation and structural number which can be seen as a proportional constant K in Preston's equation once the two parameters are determined. Based on the analysis in Section 2.2, it can be seen that $RV_1 + RV_2$ is affected by the pressure P. After simplification, Eq. (47) can be transformed into another form as follows:

$$H_t = \frac{dz}{dt} = KPV \tag{48}$$

This is the well-known Preston model. This theoretical model in this paper is in agreement with the Preston's equation and can be seen as a more comprehensive model of the Preston's equation.

4 Model validation

The data used for model validation is from the experiments conducted in literature [23]. The experimental platform is a cylindrical CNC polishing machine, the workpiece is an A356 alloy wheel and the polishing tool is a rubber belt wheel. The other parameters are shown in Table 3 and the meaning of the parameters can be seen in the appendix. The contour graph PGI830 is used to detect the profile shape of the polishing spot before and after polishing and the absolute value of the difference is calculated and taken as the actual removal depth of the workpiece.

The relationship between the depth of indentation m and the normal polishing force F is shown in Fig. 9. As we can see there is an increase in the indentation depth with the increase of the polishing force on the whole. The increment speed of the depth of indentation varies under different forces. The bigger the force is, the slower the increment speed becomes.

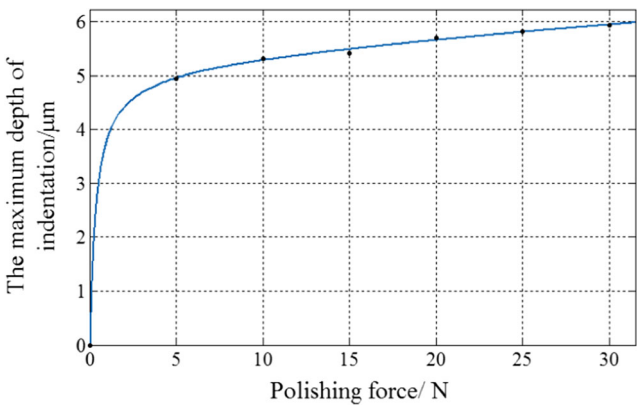

Fig. 9 The relationship between indentation depth and the force

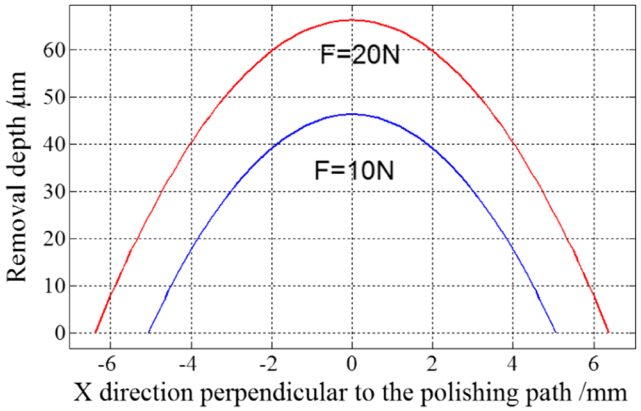

Fig. 10 The removal depth of the workpiece for different F

The reason is that as the force becomes bigger, the depth of indentation will also turn bigger. Therefore more and more abrasive grains will participate in the polishing process and undertake the force which makes the increment speed slow.

Figure 10 shows the effect of different forces F on the removal profile of the workpiece surface ($V_t = 7.540$ m/min, $V_f = 0.105$ m/min). It can be found that, with the increasing of force, the width and depth of the material removal profile increase correspondingly. The reason is that, as the force increases, the grain cutting depth into the workpiece increases too, which leads to an increased contact area as well as the number of cutting grains, thus, the width and depth of the removal profile increase. Different removal profiles under different feed rates ($F = 20$ N, $V_t = 7.540$ m/min) and polishing tool rotation speeds ($F = 20$ N, $V_f = 0.105$ m/min) are shown in Figs. 11 and 12, respectively. It can be seen that the removal depth increases when the feed rate decreases as well as the rotation speed increases, while the width of the removal profile is unchanged. This can be explained by that the decrease of feed rate or the increase of the rotation speed will increase the number of grains involved in polishing per unit time, leading to the increase of material removal volume which will finally increase the removal depth

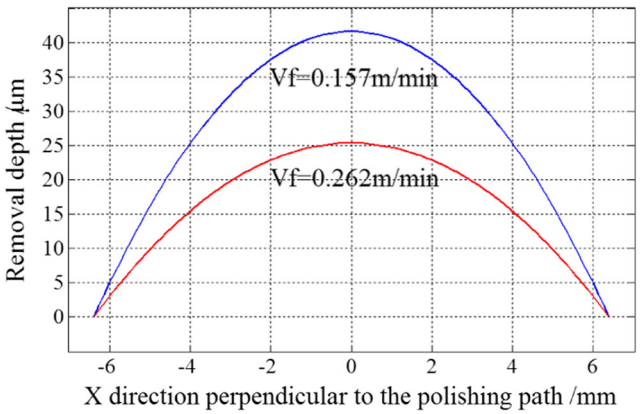

Fig. 11 The removal depth of the workpiece for different V_f

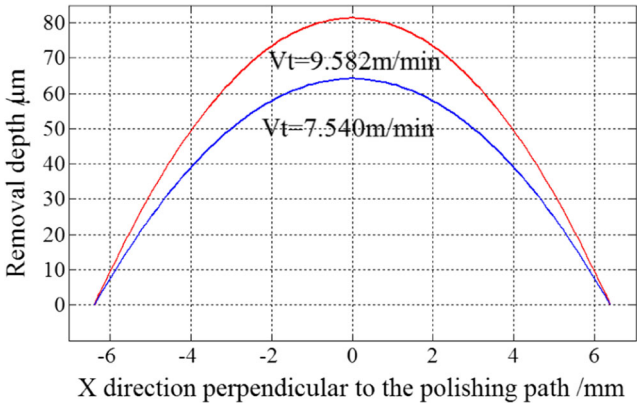

Fig. 12 The removal depth of the workpiece for different V_t

accordingly [26]. However, the feed rate and the rotation speed have little effect on the contact between the polishing tool and the workpiece, therefore the width of the profile shape is unchanged [11].

The experimental results and the predicted values of the material removal depth at the center point of contact area are shown in Table 4. They show a good agreement with each other. In addition, the predicted values using the model of this paper are compared with those using the model by Wu et al. [23], as shown in Table 4. The maximum and average relative errors by Wu et al. are 17.21 and 4.24 % which will be 11.52 and 3.11 % in the model of this paper and it shows that the model in this paper is more precise compared with the model by Wu et al., which proves the effectiveness of the model.

5 Conclusion

In this paper, a prediction model of the material removal depth for a polishing process is developed from microscopic point of view. The method of calculating the removal profile is presented. The effect of the abrasive characteristics on the depth of removal is taken into account and different stages of the polishing process are decomposed in detail. Comparison between prediction and experimental results shows a good consistency which verifies the theoretical model. The work in this paper is concluded as follows:

1. From the perspective of the grains, the proposed model takes the grit designation and structural number as the two basic variables for abrasive characteristics, and it is assumed that the shape of an abrasive grain is conic with spherical tip and the distribution of its protrusion heights is taken to be Gaussian distribution, which fully takes into account the impact of the abrasive grains characteristics on the depth of removal.
2. Different stages of the deformations of the workpiece are decomposed detailedly in the model. With the consideration that the plastic deformation is accompanied by the presence of elastic deformation, the model in this paper is more realistic.
3. Based on the theory of contact mechanics and the force equilibrium, the relationship between the pressure and the depth of indentation is obtained. Moreover, the model of the removal volume of a single abrasive grain is developed.
4. Based on the work above, the micro-model of the total removal depth for the polishing process is developed finally, which can be seen as a more comprehensive model of the Preston's equation.

The model can be used as the theoretical foundation for the selection of abrasive grains and the process parameters to achieve good form accuracy. The model proposed in this paper may be helpful for the improvement and development of the automatic polishing system.

Table 4 Comparison of the removal depth between model in this paper and other methods [23]

F (N)	V_t (m/min)	V_f (m/min)	Removal depth (10^{-3} mm)		
			Experiments	Model by Wu	Model in this paper
10	7.540	0.105	45.218	45.216	46.315
15	7.540	0.105	51.435	60.290	57.365
20	7.540	0.105	67.258	64.708	64.249
20	8.561	0.105	74.768	73.471	74.065
20	9.582	0.105	83.685	82.234	81.369
20	7.540	0.157	39.673	43.139	41.589
20	7.540	0.209	35.043	32.354	34.526
20	7.540	0.262	26.049	25.883	26.359
20	7.540	0.105	64.310	64.540	64.398
20	7.540	0.105	63.230	63.541	64.591
Maximum relative error				17.21 %	11.52 %
Average relative error				4.24 %	3.11 %

Acknowledgments This project is supported by National Natural Science Foundation of China (Grant No. 51305354).

Appendix 1: Hertzian contact theory

It is assumed that the pressure distribution between the tool and the workpiece surface is Hertzian distribution, and the contact region is a typical ellipse as shown in Fig. 11. y refers to the direction of the polishing path, a and b are the length of major semi-axis and minor semi-axis of the contact ellipse.

The pressure distribution equation is as follows:

$$p(x,y) = p_0\sqrt{1-\frac{x^2}{a^2}-\frac{y^2}{b^2}} \tag{49}$$

where p_0 is the maximum contact pressure located at the center of the contact ellipse. p_0, a and b can be calculated as follows:

$$p_0 = \frac{3F}{2\pi ab} \tag{50}$$

$$a = \left[\frac{3k_2^2\varepsilon(k_1)F}{\pi E_1^*(A+B)}\right]^{1/3} \tag{51}$$

$$b = \left[\frac{3\varepsilon(k_1)F}{\pi k_2 E_1^*(A+B)}\right]^{1/3} \tag{52}$$

where F is the applied force between the tool and the workpiece surface, E_1^* is the contact modulus of the workpiece and tool which can be given by $\frac{1}{E_1^*} = \frac{1-\nu_1^2}{E_1} + \frac{1-\nu_2^2}{E_2}$, E_1 and ν_1 refer to the Young's modulus and Poisson's ratio of the polishing tool. The other parameters can be calculated as follows:

$$k_1 = \frac{a}{b} \approx 1.0339\left(\frac{B}{A}\right)^{0.636} \tag{53}$$

$$\varepsilon(k_1) = 1.0003 + 0.5968\left(\frac{A}{B}\right) \tag{54}$$

$$A+B = \frac{1}{2}\left(\frac{1}{r_1}+\frac{1}{r_1'}+\frac{1}{r_2}+\frac{1}{r_2'}\right) \tag{55}$$

$$B-A = \frac{1}{2}\sqrt{\begin{array}{l}\left(\frac{r_1'-r_1}{r_1 r_1'}\right)^2+\left(\frac{r_2'-r_2}{r_2 r_2'}\right)^2 \\ +2\left(\frac{r_1'-r_1}{r_1 r_1'}\right)\left(\frac{r_2'-r_2}{r_2 r_2'}\right)\cos 2\gamma\end{array}} \tag{56}$$

where r_1 and r_1' are the principal radius of curvature of the polishing tool at the contacting point, r_2 and r_2' are the principal radius of curvature of the workpiece at the contacting point, γ is the included angle between the directions of principle curvature of the workpiece and tool at the contacting point.

References

1. Huissoon JP, Ismail F, Jafari A, Bedi S (2002) Automated polishing of die steel surfaces. Int J Adv Manuf Tech 19(4):285–290
2. Tsai MJ, Huang JF (2006) Efficient automatic polishing process with a new compliant abrasive tool. Int J Adv Manuf Tech 30(9-10):817–827
3. Furukawa T, Rye DC, Dissanayake M, Barratt AJ (1996) Automated polishing of an unknown three-dimensional surface. Robot Com-Int Manuf 12(3):261–270
4. Sun Y, Feng D, Guo D (2015) An adaptive uniform toolpath generation method for the automatic polishing of complex surfaces with adjustable density. Int J Adv Manuf Tech 80(9-12):1673–1683
5. Zhang L, Tam HY, Yuan CM, Chen YP, Zhou ZD (2002) An investigation of material removal in polishing with fixed abrasives. Pro Inst Mech Eng, Part B: J Eng Manuf 216(1):103–112
6. Lin SC, Wu ML (2002) A study of the effects of polishing parameters on material removal rate and non-uniformity. Int J Mach Tool Manu 42(1):99–103
7. Wang G, Zhou X, Yang X, Zhou H, Chen G (2015) Material removal profile for large mould polishing with coated abrasives. Int J Adv Manuf Tech 80(1-4):625–635
8. Preston FW (1927) The theory and design of plate glass polishing machines. J Soc Glass Tech 11:214–256
9. Zeng X, Ji SM, Tan DP, Jin MS, Wen DH, Zhang L (2013) Softness consolidation abrasives material removal characteristic oriented to laser hardening surface. Int J Adv Manuf Tech 69(9-12):2323–2332
10. Yang MY, Lee HC (2001) Local material removal mechanism considering curvature effect in the polishing process of the small aspherical lens die. J Mater Process Tech 116(2):298–304
11. Lei Z, Chuming Y, ZuDe Z (2002) Modeling and experiment of material removal in polishing on mold curved surfaces. Chin J Mech Eng 38(12):98–102
12. Wu X, Kita Y, Ikoku K (2007) New polishing technology of free form surface by GC. J Mater Process Tech 187:81–84
13. Tsai MY, Wang SM, Tsai CC, Yeh TS (2015) Investigation of increased removal rate during polishing of single-crystal silicon carbide. Int J Adv Manuf Tech 80(9-12):1511–1520
14. Wu C, Ding H, Chen Y (2009) Research on modeling method of material removal depth in CNC mechanical polishing for aluminum alloy wheel. China Mech Eng 20(21):2558–2562
15. Wang G, Wang Y, Xu Z (2009) Modeling and analysis of the material removal depth for stone polishing. J Mater Process Tech 209(5):2453–2463
16. Zhao Y, Chang L (2002) A micro-contact and wear model for chemical–mechanical polishing of silicon wafers. Wear 252(3): 220–226
17. Yeh HM, Chen KS (2010) Development of a pad conditioning simulation module with a diamond dresser for CMP applications. Int J Adv Manuf Tech 50(1-4):1–12
18. Konstantinos S, Apostolos F, George C (2014) Abrasive material. CIRP Encyclopedia of Production Engineering 1-6. Doi:10.1007/978-3-642-20617-7.
19. Xi F, Zhou D (2005) Modeling surface roughness in the stone polishing process. Int J Mach Tool Manu 45(4):365–372
20. Doman DA, Warkentin A, Bauer R (2006) A survey of recent grinding wheel topography models. Int J Mach Tool Manu 46(3): 343–352
21. Hou ZB, Komanduri R (2003) On the mechanics of the grinding process—Part I: stochastic nature of the grinding process. Int J Mach Tool Manu 43(15):1579–1593
22. Lal GK, Shaw MC (1975) The role of grain tip radius in fine grinding. J Manuf Sci E 97(3):1119–1125

23. Wu C, Ding H, Chen Y (2011) Research on modeling method of relation between abrasive grain and material removal depth. China Mech Eng 22(3):300–304
24. Xie Y, Williams JA (1996) The prediction of friction and wear when a soft surface slides against a harder rough surface. Wear 196(1): 21–34
25. Chang WR, Etsion I, Bogy DB (1987) An elastic-plastic model for the contact of rough surfaces. J Tribol 109(2):257–263
26. Ding H (2010) Basic research on process optimization for CNC mechanical polishing aluminum alloy wheel. Dissertation, Huazhong University of Science and Technology